Nucleotide-gated K_ATP channels integrated with creatine and adenylate kinases: Amplification, tuning and sensing of energetic signals in the compartmentalized cellular environment

Vitaliy A. Selivanov, **Alexey E. Alekseev**, **Denice M. Hodgson**, **Petras P. Dzeja**, and **Andre Terzic**
Division of Cardiovascular Diseases, Departments of Medicine, Molecular Pharmacology and Experimental Therapeutics, Mayo Clinic, Guggenheim, Rochester, MN, USA

Abstract

Transmission of energetic signals to membrane sensors, such as the ATP-sensitive K^+(K_{ATP}) channel, is vital for cellular adaptation to stress. Yet, cell compartmentation implies diffusional hindrances that hamper direct reception of cytosolic energetic signals. With high intracellular ATP levels, K_{ATP} channels may sense not bulk cytosolic, but rather local submembrane nucleotide concentrations set by membrane ATPases and phosphotransfer enzymes. Here, we analyzed the role of adenylate kinase and creatine kinase phosphotransfer reactions in energetic signal transmission over the strong diffusional barrier in the submembrane compartment, and translation of such signals into a nucleotide response detectable by K_{ATP} channels. Facilitated diffusion provided by creatine kinase and adenylate kinase phosphotransfer dissipated nucleotide gradients imposed by membrane ATPases, and shunted diffusional restrictions. Energetic signals, simulated as deviation of bulk ATP from its basal level, were amplified into an augmented nucleotide response in the submembrane space due to failure under stress of creatine kinase to facilitate nucleotide diffusion. Tuning of creatine kinase-dependent amplification of the nucleotide response was provided by adenylate kinase capable of adjusting the ATP/ADP ratio in the submembrane compartment securing adequate K_{ATP} channel response in accord with cellular metabolic demand. Thus, complementation between creatine kinase and adenylate kinase systems, here predicted by modeling and further supported experimentally, provides a mechanistic basis for metabolic sensor function governed by alterations in intracellular phosphotransfer fluxes.

Keywords

ATP-sensitive K^+ channel; nucleotide diffusion; metabolic sensor; intracellular compartment; heart

Metabolic sensing by K_ATP channels

Maintenance of homeostasis requires efficient transmission of energetic signals from sites of ATP generation to ATP sensors governing cellular response [1-6]. In the compartmentalized cell environment, energetic signaling must integrate detection, amplification and delivery of metabolic signals arising from deviations in adenine nucleotide levels [1-9]. While the identity of energy-responsive elements is being increasingly resolved, the molecular mechanisms that synchronize metabolic sensor function with cell metabolism remain largely unknown.

ATP-sensitive K^+ (K_{ATP}) channels are membrane metabolic sensors that adjust membrane excitability depending on the cellular energetic status [10-12]. K_{ATP} channels are expressed in metabolically active tissues, such as the heart, where the pore-forming Kir6.2 protein assembles with the regulatory sulfonylurea receptor SUR2A subunit to form functional channels (Fig. 1) [13-15]. ATP maintains K_{ATP} channel closure by binding to Kir6.2 [16,17], whereas ATP/ADP interactions with SUR secure the metabolic sensor function of the channel complex (Fig. 1A) [18-20]. The sensor role of cardiac K_{ATP} channels stems from the non-equivalent properties of nucleotide binding domains (NBD1 and NBD2) in the SUR2A subunit (Fig. 1A). NBD1 binds nucleotides whereas NBD2 hydrolyzes ATP, with NBDs working in tandem to gate K_{ATP} channels [21-23]. The ATP hydrolysis cycle at SUR2A drives conformational transitions with distinct outcomes on channel gating imparting low or high ATP-sensitivity to the channel [24]. Increase in MgADP under stress stabilizes the channel in a conformation associated with reduced sensitivity to ATP, conferring allosteric regulation to K_{ATP} channels [24].

Allosteric nucleotide-dependent channel gating implies that K_{ATP} channels adopt highest sensitivity to ATP in the absence of ADP, and are converted to their lowest ATP-sensitivity by MgADP (Figs 1B and 1C). Although the MgADP-bound state of SUR shifts the range for ATP inhibition (IC_{50} from 30-300 μM), this remains far below intracellular ATP levels (Fig. 1B). On saturating all ADP-binding sites, at > 100 μM ADP, no further reduction in ATP sensitivity can be achieved (Fig. 1C) [25, 26], implying that MgADP-dependent K_{ATP} channel regulation is insufficient for channel gating at normally high cytosolic concentrations of ATP (6-10 mM) [27, 28]. Rather, K_{ATP} channels could sense local nucleotides set by ATPases in the submembrane space at a level distinct from that of the `bulk' cytosol [25, 29, 30], provided there exist significant diffusional limitations between the two cellular compartments. Yet, compartmentalization [9, 31] would hamper recognition of energetic signals by K_{ATP} channels, as channel gating would be relegated to local fluctuations of nucleotides. Therefore, in a compartmentalized cell, adequate K_{ATP} channel regulation requires transmission of energetic signals across diffusional barriers, and translation into a local nucleotide change sufficient for channel activation. However, signal translation should not trigger uncontrolled current flow through K_{ATP}channels that would arrest membrane excitation by clamping the resting potential of cells at the K^+ equilibrium. Thus, energetic signaling to the channel must be managed by systems capable not only to `amplify', but also `tune' nucleotide signals in order to selectively secure beneficial channel activity in accord with cellular metabolic demand.

Cells with high and fluctuating energy demands possess catalyzed phosphotransfer circuits that facilitate energy transfer between sites of ATP production and utilization [2,5,11,32-35]. Isoforms of phosphotransfer enzymes, adenylate kinase (AK) and creatine kinase (CK), are found in distinct cellular compartments, including membranes where K_{ATP} channels reside [11,33]. A role for AK and CK, along with glycolytic reactions, in modulating K_{ATP} channel activity was inferred from the redistribution of cellular phosphotransfer in response to metabolic challenge [2,30,32,36]. In fact, AK and CK substrates regulate nucleotide-dependent K_{ATP} channel gating, a property lost on deletion of *AK1* or *M-CK* genes that encode major AK and CK isoforms (Fig. 2) [11,24,33,34]. Intimate relationships between individual phosphotransfer enzymes and the channel itself, as well as the requirement for phosphotransfer systems in synchronizing metabolic sensing with cellular energetics have been also demonstrated [11,24,34,37,38]. However, coordination of AK and CK phosphotransfer, and their respective roles in securing transmission of metabolic signals to the metabolic sensor have not been defined.

K$_{ATP}$ channel gating and AK-catalyzed nucleotide conversion in the submembrane compartment

By virtue of nucleotide sensitivity, K$_{ATP}$ channels provide a fine gauge of energetic dynamics in the submembrane microenvironment [24,34], Opening of just 1 % of the channel population is an established threshold above which significant contribution of K$_{ATP}$ channels to membrane excitability can be expected [25,30,39]. This could occur at submembrane ATP < 3 mM and saturating ADP > 300 μM (Fig. 3A). Provided that nucleotide mobility between cytosolic and submembrane compartments is limited [31], these submembrane nucleotide levels could be generated by membrane ATPases [30,39] including ATP hydrolysis by the K$_{ATP}$ channel [22,24], as well as AK (ATP + AMP $\leftrightarrow$ 2 ADP; Fig. 3A).

At steady-state, ATPase flux (J_{ATPase}) in the submembrane compartment is equal to ATP diffusional flux (J_{ATP}) into the submembrane space plus local ATP production by AK (Fig. 3B). As AMP is co-produced in the AK reaction, AK-catalyzed ATP generation in the submembrane can be expressed as diffusion of AMP into bulk space (-J_{AMP}). Thus, ATPase flux equals:

$$J_{ATPase} = -J_{AMP} + J_{ATP} \tag{1}$$

Sarcolemmal ATPase flux was previously derived from total ATPase activity in working hearts (300 nmol/min/mg protein; [34]), assuming that 120 mg of protein (with 1 mg of sarcolemmal protein) is contained in 1 g of tissue and that ~ 5% of total energy is consumed by sarcolemmal ATPases [40]. Thus, ATPase activity:

$$300 \quad \text{nmol/min/mg protein} \times 120 \quad \text{mg/g wet wt} \times 0.05 = 1800 \quad \text{nmol/min/g wet wt} = 0.03 \mu\text{mol/s/g wet wt}$$

ATPase activity can be converted into flux units (μmol/cm^2/s) provided the total sarcolemmal surface in 1 cm^3 of tissue (1 g wet wt). For a cardiomyocyte (5 × 10 × 60 μm) with a volume of 3000 μm^3, the amount of cells in 1 cm^3 is 3.33 × 10^8 per g wet wt with a surface of:

$$3.33 \times 10^8 \times 2 \times (5 \times 10 + 5 \times 60 + 10 \times 60) \mu m^2/g \quad \text{wet wt} = 6330 \quad cm^2/g \quad \text{wet wt.}$$

Thus, sarcolemmal ATPase flux is:

$$0.03 \quad \mu\text{mol/s/g wet wt} \div 6330 \quad cm^2/g \text{ wet wt} = 4.7 \quad 10^{-6} \mu\text{mol/cm}^2/s.$$

Nucleotide diffusion (with the same coefficient D for all nucleotides) can be described according to Fick's law as one-dimensional flux (through total cell area in 1 g of tissue, S) perpendicular to the membrane. For ATP:

$$J_{ATP}(x) = -DS \frac{\partial [ATP(x)]}{\partial x}$$

where $J_{ATP}(x)$ is ATP flux at distance x. At steady-state, with fluxes constant along x:

$$J_{ATP} = \frac{-DS}{\Delta x} \Delta ATP, \quad J_{ADP} = \frac{-DS}{\Delta x} \Delta ADP, \quad J_{AMP} = \frac{-DS}{\Delta x} \Delta AMP \tag{2}$$

where $\Delta ATP = [ATP]_b - [ATP]_m$, i.e. the difference in ATP concentration between the cytosolic bulk ($_b$) and subsarcolemmal ($_m$) space. Diffusional fluxes for ADP and AMP (J_{ADP}, J_{AMP}) are described analogously. The thickness of the submembrane compartment, Δx is 0.2 μm [34].

At AK equilibrium in the cytosol $\left(K_{AK} = [ATP]_b [AMP]_b / [ADP]_b^2 = 1\right)$, bulk ADP and AMP are expressed through total nucleotide pool ([TNP]) and $[ATP]_b$ as:

$$[ADP]_b = \frac{\left(-[ATP]_b + \sqrt{[ATP]_b^2 + 4[TNP][ATP]_b \ K_{AK} - 4[ATP]_b^2 \ K_{AK}}\right)}{2K_{AK}}$$

(3)

$$[AMP]_b = [TNP] - [ATP]_b - [ADP]_b$$

At steady-state nucleotide fluxes $J_{ATP} + J_{AMP} + J_{ADP} = 0$ thus using Eq. 2:

$$\Delta ATP + \Delta ADP + \Delta AMP = 0$$

(4)

At AK equilibrium in the submembrane compartment:

$$K_{AK} = \frac{([ATP]_b - \Delta ATP)([AMP]_b - \Delta AMP)}{([ADP]_b - \Delta ADP)^2},$$

(5)

based on the interrelationship between nucleotide concentrations and fluxes (Eqs 1 and 4) the diffusion coefficient D can be derived as:

$$= -\frac{\Delta x J_{ATPase}\left(-\Delta ATP + 2[ADP]_b K_{AK} + 4K_{AK}\Delta ATP + [ATP]_b + \sqrt{-(\Delta ATP - [ATP]_b)(\Delta ATP(4K_{AK} - 1) + 4K_{AK}([ADP]_b + [AMP]_b) + [ATP]_b)}\right)}{2\left([ADP]_b^2 K_{AK} + \Delta ATP^2(4K_{AK} - 1) + \Delta ATP(4[ADP]_b K_{AK} + [AMP]_b) + [ATP]_b(\Delta ATP - [ADP]_b)\right)}$$

where $[ADP]_b$ and $[AMP]_b$ are defined by Eq. 3. At [TNP] = 7 mM and $[ATP]_b$ = 6.99 mM [27,28,34], the diffusion coefficient D must be 1.5 10^{-11} cm^2/s to provide a 4 mM ΔATP, and thereby 3 mM $[ATP]_m$ necessary for merest K_{ATP} channel activity (Fig. 3A). This diffusion coefficient is in line with other estimates for diffusion of nucleotides in a cell, and indicates strong diffusion barriers between cellular compartments [34,41,42].

The lower value of D obtained here in the presence of AK, compared to D = 2.3 10^{-11} cm^2/s reported previously in the absence of AK [34], underscores the significance of this enzyme in reducing ATP and ADP gradients between cell compartments. Actual nucleotide gradients at different bulk ATP levels can be obtained by solving Eqs 1, 2, 4 and 5:

$$\Delta ATP = -\frac{2[ADP]_b}{3} - \frac{[AMP]_b}{6} - \frac{[ATP]_b}{6} + \frac{\Delta x J_{ATPase}}{2D} + \frac{1}{12D^2} \times$$
$$\times \left\{ D^4(-8[ADP]_b - 2[AMP]_b - 2[ATP]_b)^2 - 12D^2 \times \right.$$
$$\left. \left(4[ADP]_b^2 + 2D\Delta x[AMP]_b J_{ATPase} + \Delta x^2 J_{ATPase}^2 - 4D^2[AMP]_b[ATP]_b - 2D\Delta x J_{ATPase}[ATP]_b\right) \right\}^{1/2}$$

(6)

$$\Delta ADP = -\frac{2D\Delta ATP - \Delta x J_{ATPase}}{D}$$

$$\Delta AMP = -\Delta ATP - \Delta ADP$$

with bulk ADP and AMP levels defined by Eq. 3, at K_{AK}=1.

The nucleotide gradient for ATP is significantly lower in the presence (Eq. 6) than in the absence (Eq. 2) of AK (Fig. 3C). Computation of submembrane nucleotide concentrations (Eqs 3 and 6) revealed that AK effectively buffered ATP level at the membrane despite significant changes in bulk ATP (Fig. 3D) or ATPase flux (Fig. 3E). In the absence of AK, the strong diffusion barrier between compartments would promote disappearance of submembrane ATP following minor drop in bulk ATP levels (i.e. from 6.99 to 6.65 mM as shown in Fig. 3D). AK, present in the vicinity of K_{ATP} channels [11,33], could serve as a `rectifying device' capable of `flattening' metabolic signals. Following a 2 mM drop in bulk ATP (from 7 to 5 mM), AK would halve changes in submembrane ATP (Fig. 3D). Moreover, local nucleotide fluctuations induced by changes in membrane ATPase activity would also be smoothed by the AK system (Fig. 3E).

Thus, in the submembrane compartment of cardiac cells, with ongoing ATP consumption and restricted nucleotide diffusion, active AK could buffer $[ATP]_m$ and $[ADP]_m$, protecting channel activity from oscillations in bulk nucleotides or membrane ATPase activity. In this way, AK would attenuate alterations in the $[ATP]_m/[ADP]_m$ ratio, requiring a complementary mechanism for effective energetic signal transmission between compartments.

CK-facilitated nucleotide diffusion in the compartmentalized cellular environment

The dynamics of CK flux are tightly coupled to cellular metabolism, implicating CK in energetic communication between cell compartments [34,35,43]. To estimate the contribution of the creatine phosphate/CK system in signal transduction over the diffusional barrier, diffusion of nucleotides, creatine (Cr), and creatine phosphate (CrP) between cell compartments was considered in conjunction with the CK reaction (ADP + CrP ↔ ATP + Cr) integrated with membrane ATPase activity (Fig. 4A). Therefore, CK flux corresponds to diffusional CrP flux (J_{Crp}), and at steady-state ATPase flux equal the ATP plus CrP diffusional fluxes:

$$J_{ATPase} = J_{CrP} + J_{ATP} \tag{7}$$

Diffusion of Cr and CrP can be described analogously to nucleotide fluxes (Eq. 2):

$$J_{Cr} = \frac{-D_{Cr}S}{\Delta x}\Delta Cr, J_{CrP} = \frac{-D_{Cr}S}{\Delta x}\Delta_{CrP}, \tag{8}$$

where the diffusion coefficient D_{Cr} is assumed equal for both Cr and CrP, $\Delta x = 0.2$ μm. Since Cr and CrP diffuse in the aqueous phase 1.5 times faster than nucleotides, $D_{Cr} = 1.5D = 2.25 \times 10^{-11}$ cm^2/s. Further, the equilibrium constant of the CK reaction:

$$K_{CK} = \frac{[ATP]_b [Cr]_b}{[ADP]_b [CrP]_b} = 160,$$

(9)

at pH = 7, in the presence of 1 mM Mg^{2+} [43]. At equilibrium, defining total bulk concentration for Cr plus CrP [CrT] = 40 mM [44], and total bulk nucleotide pool [*TNP*], it follows from Eq. 9:

$$[CrP]_b = \frac{([CrT][ATP]_b)}{[TNP] + [ATP]_b - K_{CK}[ATP]_b}$$

(10)

$$[Cr]_b = [CrT] - [CrP]_b$$

$$[ADP]_b = [TNP] - [ATP]_b$$

At steady-state, total adenine nucleotide flux and total Cr/CrP flux, imply, due to Eqs 2 and 8, that

$$\Delta ATP + \Delta ADP = 0 \text{ and } \Delta CrP + \Delta Cr = 0$$

(11)

Considering CK equilibrium in the membrane vicinity

$$\overline{([ADP]_b - \Delta ADP)([CrP]_b - \Delta CrP),}$$

(12)

and the relationships between concentrations (Eq. 11) and fluxes (Eqs 2, 7 and 8), values of ΔATP, ΔADP, ΔCr and ΔCrP can be derived as Eq. 13 (see bottom of page).

$\Delta Cr = -\Delta CrP$, where $[CrP]_b$, $[Cr]_b$ and $[ADP]_b$ are defined by Eq. 10.

At high $[ATP]_b$, CK in the membrane vicinity would scavenge ADP, and strongly support ATP levels. In stress, assuming a 1.5 mM decrease in bulk ATP, the profile of ΔATP, constructed as a function of $[ATP]^b$ based on Eq. 13, predicts a ~ 6 mM drop in submembrane ATP coupled with an equivalent increase in $[ADP]_m$ (Figs 4B and 4C). This steep slope of ΔATP is accompanied by abrupt decline in submembrane CrP. Due to diffusional restrictions, a drop in $[ATP]_b$ from 6.99 to 6.5 mM would induce a major (~ 23 mM) drop of $[CrP]_m$ (Fig. 4B; Eq. 13). In contrast to AK, CK loses its effectiveness to maintain low ΔATP upon minor drop in $[ATP]_b$ amplifying changes of bulk ATP into large alterations of nucleotide content at the submembrane. However, active CK in conjunction with AK would blunt membrane ATPase-induced nucleotide fluctuations in the submembrane (Fig. 4D) protecting membrane sensors from background metabolic noise. Thus, the ability of CrP flux to carry energetic equivalents between cell compartments defines the role of CK in transmitting and amplifying metabolic signals.

Metabolic signaling in the compartmentalized cell by integrated AK and CK systems

Energy consumption by membrane ATPases integrated with CK-facilitated nucleotide diffusion and AK-catalyzed nucleotide conversion in cellular compartments (Fig. 5) can be defined at steady-state as follows:

$$J_{ATPase} = -J_{AMP} + J_{ATP} + J_{CrP} \qquad (14)$$

With CK and AK at equilibrium, and bulk concentrations of ADP, AMP, Cr and CrP derived from Eqs 2, 4, 5, 8, 9, 11, 12, 14, profiles of nucleotide gradients and the submembrane nucleotide content were computed (Fig. 6).

Within a wide range of membrane ATPase activity, cooperative action of CK and AK virtually nullified differences between bulk vs. submembrane nucleotide concentrations at a given $[ATP]_b$ (Fig. 6A). Along a co-active AK system, CK amplified cytosolic signals over the diffusion barrier separating cell compartments. Reduction by only 0.2 mM (from 6.7 mM) in $[ATP]_b$ generated a 2 mM ΔATP (Fig. 6B), with a respective drop in $[ATP]_m$ (Fig. 6C). With further reduction in bulk ATP, and decrease in CK flux (decrease of J_{CrP}), AK could keep ΔATP constant (Fig. 6B), reducing the rate of drop in $[ATP]_m$ (Fig. 6C). This is associated with augmented ΔAMP accomplished by inversion of ΔADP changes, from an initial increase at high $[ATP]_b$ to a decrease following further reduction in $[ATP]_b$ (Fig. 6B). The profile of submembrane AMP dynamics underscores the distinct efficacy of CK and AK at high vs. low $[ATP]_b$ (Fig. 6C). As long as CK effectively supports $[ATP]_m$ when oscillations of $[ATP]_b$ are minor, $[AMP]_m$ remains ~ 0 mM. Upon significant drop in $[ATP]_b$ when CK fails to maintain $[ATP]_m$, $[AMP]_m$ increases reflecting the activity of AK in support of $[ATP]_m$ (Fig. 6C).

While CK is dominant in the myocardium, reduced CK flux under stress up-regulates AK phosphotransfer [11,34,46,47]. This interplay between phosphotransfer pathways reflects specific functions for CK and AK in metabolic signal transduction [32]. Here, energetic signals, simulated as a 0.5 mM dip in $[ATP]_b$, were amplified by altered CK flux into large responses in $[ATP]_m$ and the $[ATP]_m/[ADP]_m$ ratio (Fig. 7A, upper row). AK attenuated the $[ATP]_m$ response by preserving the $[ATP]_m/[ADP]_m$ ratio (Fig. 7A, middle row). Under cooperative action, CK would secure transmission of amplified signals, while the `rectifying' function of AK would tune amplified signals (Fig. 7A, lower row). Doubling the magnitude of the signal, through step-wise drop in $[ATP]_b$, would translate into amplified response in $[ATP]_m$ yet at reduced increments, and ultimately in the ceiling of magnified $[ATP]_m/[ADP]_m$ ratio (Fig. 7A, lower row). This modulatory role of AK would preserve submembrane processes from excessive changes in nucleotides following metabolic signal transmission. The effectiveness of signal transmission, driven by CK and expressed as a derivative of ATP_m over ATP_b in response to changes in ATP_b, is insensitive to AK modulation at smaller variations in ATP_b, but becomes attenuated by AK as fluctuations in ATP_b increase (Fig. 7B).

$$
\begin{aligned}
\Delta ATP = & -\frac{1}{2D(K_{CK}-1)}\left([Cr]_b D_{Cr} + [ADP]_b K_{CK} D + [CrP]_b K_{CK} D_{Cr} + [ATP]_b D + J_{ATPase}\Delta x - K_{CK} J_{ATPase}\Delta x - \right. \\
& -\left\{ \begin{array}{l} ([Cr]_b D_{Cr} + [ADP]_b K_{CK} D + [CrP]_b K_{CK} D_{Cr} + [ATP]_b D - J_{ATPase}\Delta x + K_{CK} J_{ATPase}\Delta x)^2 - 4D_{Cr}(K_{CK}-1)\times \\ \times([CrP]_b[ADP]_b K_{CK} D - [Cr]_b[ATP]_b D + [Cr]_b J_{ATPase}\Delta x + [CrP]_b J_{ATPase} K_{CK}\Delta x) \end{array} \right\}^{1/2} \\
\Delta CrP = & -\frac{1}{2D_{Cr}(K_{CK}-1)}\left([Cr]_b D_{Cr} + [ADP]_b K_{CK} D + [CrP]_b K_{CK} D_{Cr} + [ATP]_b D - J_{ATPase}\Delta x + K_{CK} J_{ATPase}\Delta x - \right. \\
& -\left\{ \begin{array}{l} ([Cr]_b D_{Cr} + [ADP]_b K_{CK} D + [CrP]_b K_{CK} D_{Cr} + [ATP]_b D - J_{ATPase}\Delta x + K_{CK} J_{ATPase}\Delta x)^2 - 4D_{Cr}(K_{CK}-1)\times \\ \times([CrP]_b[ADP]_b K_{CK} D - [Cr]_b[ATP]_b D + [Cr]_b J_{ATPase}\Delta x + [CrP]_b J_{ATPase} K_{CK}\Delta x) \end{array} \right\}^{1/2} \\
\Delta ADP = & -\Delta ATP
\end{aligned}
\qquad (13)
$$

The role of phosphotransfer systems in signal transmission between cell compartments was assessed in permeabilized cardiomyocytes when membrane Na^+/K^+-ATPase was activated by application of 40 mM NaCl in the bath solution. K_{ATP} channel activity induced by intracellular Na^+ was sensitive to ouabain, an established inhibitor of the Na^+/K^+-ATPase (Fig. 7C, upper trace). In the absence of CK phosphotransfer, inhibition of AK by di(adenosine-5′) pentaphosphate (P^1,P^5) increased K_{ATP} channel activity (Fig. 7C, lower trace). This indicates a contribution of the AK system in the maintenance of submembrane ATP levels facilitated by AMP diffusional efflux, consistent with the demonstrated ability of AK to promote energetic communication and facilitate ATP delivery between cellular compartments [35,48].

That modulation in CK flux amplifies bulk energetic signals in the vicinity of K_{ATP} channels can be shown by the experimentally obtained relationships of ATP-induced channel inhibition measured in permeabilized cardiac cells in the presence ($J_{CK} >> 0$) and absence ($J_{CK} = 0$) of CrP (Fig. 7D). Following changes in bulk ATP level and drop in CK flux, K_{ATP} channel activity now operates at a higher probability of channel opening (Fig. 7D). This amplified channel response implies higher changes in submembrane concentrations of nucleotides in comparison to more modest alterations in the bulk space. Depending of the actual change in J_{CK} flux, in response to changes in $[ATP]^b$, K_{ATP} channel activity would be defined by an intermediate curve of ATP-induced channel inhibition (between the two extremes: $J_{CK} >> 0$ *vs.* $J_{CK} = 0$). According to the CK reaction equilibrium, through substitution by $[Cr]_b$ of 9.95 out of the total 10.25 mM of $[CrP]_b$, a 50 μM drop of $[ATP]_b$ (from 0.3 to 0.25 mM) and concomitant increase of $[ADP]_b$ is calculated to occur. According to the model prediction, this minor drop in $[ATP]_b$, which by itself is insufficient to induce channel opening, can be amplified by the altered CK flux into significant nucleotide changes in the submembrane space leading to vigorous activation of K_{ATP} channels (Fig. 7E).

Decoding of signals processed by creatine and adenylate kinase to K_{ATP} channels

As long as $[ATP]_b$ and $[ATP]_m$ are equilibrated at ~ 7 mM, by co-active CK and AK systems, K_{ATP} channels remain closed as it follows from the allosteric model of nucleotide-dependent channel gating (Eqs A1-A3 in Appendix; Fig. 8A). However, a drop in $[ATP]_b$ from 7 to 6 mM induces a drop in CrP levels and a ~ 75% reduction in CrP diffusional flux (J_{CrP}). This translates into a change in ATP_m from 7 to 3 mM (Fig. 8A) and a significant rise of $[ADP]_m$ (Fig. 6C) sufficient to activate > 1% of K_{ATP} channels necessary for action potential shortening (Fig. 8A), as experimentally observed under the metabolic stress of hypoxia [34]. In the absence of AK-dependent modulation of the transmitted signal, an extremely steep channel response to modest alterations of $[ATP]_b$ would expose the cell to excessive activation of K_{ATP} current that could arrest membrane excitability (Fig. 8B). Tuning the CK-dependent amplification of the nucleotide response can be provided by the AK system capable of adjusting the ATP/ADP ratio in the submembrane compartment, and thereby securing a more controlled regulation of K_{ATP} channel opening under stress (Figs 8A and 8B).

In addition to conditions associated with significant drop in $[ATP]_b$, it is becoming increasingly evident that cardiac K_{ATP} channels may also be active under conditions where such changes in $[ATP]_b$ are not readily detectable [49]. This may be the case of hearts exposed to the stress of catecholamine challenge, where in response to increase in heart rate and contractility, K_{ATP} channel opening is involved in homeostatic adjustment of membrane excitability [50]. In this regard, a 30-40% augmentation of membrane ATPase activity predicts an increased probability of channel opening in the absence of significant changes in $[ATP]_b$ (Fig. 8B).

While the AK-catalyzed reaction facilitates delivery and maintenance of ATP levels at ATPase sites [35,48], under metabolic stress AMP produced by AK can drive the reaction towards ADP

generation at the channel site promoting K_{ATP} channel opening [11,32,33]. Under severe stress, reversal of mitochondrial F_0F_1-ATP synthase into an ATPase associated with significant lowering of mitochondrial and cytosolic ATP, would drive the AK reaction towards AMP production. Elevated AMP in the submembrane compartment, in the presence of a local ATP regenerating system such as glycolysis or an external source of ATP that could support $[ATP]_m$ above $[ATP]_b$, would promote $[ADP]_m$ generation ($ATP + AMP \rightarrow 2\,ADP$) facilitating K_{ATP} channel opening (Fig. 8C). Such a condition can be simulated in permeabilized cardiomyocytes using dinitrophenol (DNP), a mitochondrial uncoupler. DNP-induced K_{ATP} channel activation is antagonized by P^1,P^5, an AK inhibitor, in wild-type cardiomyocytes, but not in AK1-knockout cardiac cells, lacking the major AK isoform (Fig. 8D) [11]. Thus, under these conditions of metabolic stress, the AK reaction would promote $[ATP]_m$ removal and $[ADP]_m$ generation required for K_{ATP} channel opening (Fig. 8D), in line with the plasticity of phosphotransfer-mediated signaling between cellular compartments.

Summary

Energetic signal transduction is a vital homeostatic process, yet the fundamental mechanisms governing transmission, decoding and sensing are partially understood. Here, using cardiac K_{ATP} channels as prototypic membrane metabolic sensors, we analyzed principles determining transmission and detection of metabolic signals in the compartmentalized cellular environment. The presented model revealed that energetic signals, simulated as deviation of bulk ATP from its basal level, when transmitted over the diffusional barrier into the submembrane space, modify local nucleotide levels. Signal transmission from the cytosol to the submembrane compartment would be limited due to restricted diffusion of nucleotides, Cr and CrP. However, facilitated diffusion provided by CK and AK phosphotransfer systems essentially dissipated nucleotide gradients imposed by membrane ATPases and diffusional restrictions, coupling K_{ATP} channels with cellular metabolism. Under stress, even with a moderate drop in $[ATP]_b$, CK could no longer effectively dissipate nucleotide gradients precipitating a significant fall in $[CrP]^m$, and generating an amplified nucleotide response at the K_{ATP} channel site. CK-dependent amplification of the nucleotide response was tuned by the AK system capable of attenuating changes in the ATP/ADP ratio in the submembrane compartment, thereby securing transmission of controllable metabolic signals to K_{ATP} channels. Under severe metabolic challenge, provided that a local regenerating system maintained submembrane ATP levels, AK catalysis could promote the response of the membrane metabolic sensor. Thus, energetic signals generated in the cytosol are processed through CK and AK systems, which provide a mechanistic basis for synchronization of K_{ATP} channel function with cellular metabolism.

The proposed mechanism, predicted by modeling and supported experimentally, integrates only two major phosphotransfer enzymes, CK and AK, without including other energy converting systems, such as glycolysis, which could modulate the local nucleotide content [29,32]. In fact, active glycolysis would scavenge ADP produced by membrane ATPases maintaining local ATP/ADP ratios and modulating apparent ATPase flux. Furthermore, CK, AK and glycolytic systems appear closely interrelated as drop in CK flux and increase in AK catalysis under stress is associated with concomitant activation of glycolytic flux [30,34,36, 46,51]. Detailed analysis of the glycolytic contribution requires consideration of the complex kinetics of nucleotide modulation at a local level since ATP consumption at initial glycolytic steps could augment, while ATP produced in later steps of glycolysis would diminish the local nucleotide response. In response to a shift of bulk ATP, the presented model predicts a millimolar accumulation of ADP in the submembrane space that, in turn, can slow the rate of the membrane ATPase reaction [52]. In this way, signaling-induced alterations in submembrane ADP could affect not only gating of K_{ATP} channels but also other membrane energy consuming systems. Thus, changes in glycolytic and membrane ATPase activity, induced by the signal transmitted into the submembrane space, represent a feedback

mechanism bringing an additional mode to the dynamics of the nucleotide response, which requires further refinement of the proposed model.

Although throughout the present analysis AK and CK reactions were considered at equilibrium in order to minimize the number of unknown parameters, recent findings suggest that in an ATP-consuming cellular compartment the CK reaction could operate out of equilibrium indicative of an insufficiency of the CK system in compensating local ATPase flux [53]. In fact, increment in cardiac work shifts the CK reaction further from equilibrium [53], and could accentuate a drop in $[ATP]_m$. Therefore, the effectiveness of metabolic signal transmission at non-equilibrium could be even higher in comparison with signal amplification produced by reactions at equilibrium.

The presented model does not consider the kinetics of diffusional fluxes, nor the kinetics of enzymatic reactions, and assumes that changes in cytosolic adenine nucleotide levels are sufficiently sustained or occur slowly enough, so that the respective steady-state in the submembrane space is reached. It is conceivable that fast rate changes in bulk nucleotides could not be detected, amplified or transmitted, and thus would be filtered out by slower kinetic processes. Although K_{ATP} channels can respond to oscillations in cellular metabolism [2], lack of detectable K_{ATP} channel-dependent contribution to action potential duration in normal heart [49,50,54] indicates that the intracellular signal transmission system apparently does not communicate to the channel site brief changes in ATP levels during the cardiac contractile cycle [55]. Thus, at high diffusional limitations, the characteristic time of the response to a cytosolic signal should exceed the cardiac contractile cycle itself. In this regard, only sustained changes in cellular energetics would be communicated producing a K_{ATP} channel response, yet the time course of signal transmission needs to be evaluated.

In summary, intercommunication between the CK and AK phosphotransfer pathways could underlie metabolic signal transmission and amplification to cardiac K_{ATP} channels, in line with channel function under conditions of normal and stressed cellular energetics [11,34,50]. This framework is a step towards the elucidation of metabolic sensor function that would take into account phosphotransfer reactions in conjunction with other metabolic signal generating and processing systems translating changes in the energetic state into an integrated cellular response.

Acknowledgements

Appendix

Allosteric model of channel gating

Nucleotide-dependent K_{ATP} channel gating was simulated by an allosteric model where: (i) 4 identical binding sites for ATP and ADP co-exist within the octameric stoichiometry of the K_{ATP} channel complex [15,19]; (ii) binding of ATP to the pore-forming Kir6.2 subunit inhibits channel opening [16,17]; (iii) binding of ADP to the regulatory SUR subunit antagonizes ATP-binding to Kir6.2 [18,20,21]. T_i and D_i (i = 0-4) are channel species with bound ATP and/or ADP. k_0 and k_1 are dissociation constants for ATP binding to Kir6.2 in the absence and presence of ADP at the associated SUR. k_{ADP} is the dissociation constant of ADP from SUR, independent from ATP binding. Distribution of channel species with 0-4 ADP bound molecules was:

$$\frac{D_1}{D_0} = \frac{4 \cdot [ADP]}{k_{ADP}}; \frac{D_2}{D_1} = \frac{3 \cdot [ADP]}{2k_{ADP}}; \frac{D_3}{D_2} = \frac{2 \cdot [ADP]}{3k_{ADP}}; \frac{D_4}{D_3} = \frac{[ADP]}{4k_{ADP}}; \sum_{j=t}^{4} D_j = 1 \tag{A1}$$

with the percentage of D_i species expressed as a function of ADP concentration:

$$\overline{k_{ADP}}; D_3 = 4 \cdot D_0 = ([ADP]^3 \ \overline{k_{ADP}}; D_4 = D_0 = ([ADP]^4 \ \overline{k_{ADP}}, \tag{A2}$$

where

$$D_0 = 1 + \left\{ \frac{4 \cdot [ADP]}{k_{ADP}} + 6 \cdot \left(\frac{[ADP]}{k_{ADP}} \right)^2 + 4 \cdot \left(\frac{[ADP]}{k_{ADP}} \right)^3 + \left(\frac{[ADP]}{k_{ADP}} \right)^4 \right\}^{-1}$$

The following system of equations described the distribution of channel species with 0 to 4 ATP bound molecules taking into account that ATP binding is dependent on ADP:

$$\frac{T1_{D0}}{T0_{D0}} = \frac{4 \cdot [ATP]}{k_0}; \frac{T2_{D0}}{T1_{D0}} = \frac{3 \cdot [ATP]}{2k_0}; \frac{T3_{D0}}{T2_{D0}} = \frac{2 \cdot [ATP]}{3k_0}; \frac{T4_{D0}}{T3_{D0}} = \frac{[ATP]}{4k_0}; \sum_{i=1}^{4} Ti_{D0} = D_0$$

$$\frac{T1_{D1}}{T0_{D1}} = \frac{3 \cdot [ATP]}{k_0}; \frac{T2_{D1}}{T1_{D1}} = \frac{[ATP]}{2k_0}; \frac{T3_{D1}}{T2_{D1}} = \frac{[ATP]}{3k_0}; \frac{T4_{D1}}{T3_{D1}} = \frac{[ATP]}{4k_0}; \sum_{i=1}^{4} Ti_{D1} = D_1$$

$$\frac{T1_{D2}}{T0_{D2}} = \frac{2 \cdot [ATP]}{k_0}; \frac{T2_{D2}}{T1_{D2}} = \frac{[ATP]}{2k_0}; \frac{T3_{D2}}{T2_{D2}} = \frac{2 \cdot [ATP]}{3k_0}; \frac{T4_{D2}}{T3_{D2}} = \frac{[ATP]}{4k_0}; \sum_{i=1}^{4} Ti_{D2} = D_2$$

$$\frac{T1_{D3}}{T0_{D3}} = \frac{[ATP]}{k_0}; \frac{T2_{D3}}{T1_{D3}} = \frac{[ATP]}{2k_0}; \frac{T3_{D3}}{T2_{D3}} = \frac{[ATP]}{3k_0}; \frac{T4_{D3}}{T3_{D3}} = \frac{[ATP]}{4k_0}; \sum_{i=1}^{4} Ti_{D3} = D_3$$

$$\frac{T1_{D4}}{T0_{D4}} = \frac{4 \cdot [ATP]}{k_1}; \frac{T2_{D4}}{T1_{D4}} = \frac{3 \cdot [ATP]}{2k_1}; \frac{T3_{D4}}{T2_{D4}} = \frac{2 \cdot [ATP]}{3k_1}; \frac{T4_{D4}}{T3_{D4}} = \frac{[ATP]}{4k_1}; \sum_{i=1}^{4} Ti_{D4} = D_4 \tag{A3}$$

k_0, k_1 and k_{ADP} were determined by fitting experimental data from ATP-induced K_{ATP} channel inhibition in the absence of ADP, at saturating ADP and at sub-saturating ADP, respectively (Fig. 1). The best data fit revealed that more than one ATP is required to close the K_{ATP} channel octamer. In the model, channel species with more than one bound ATP, thus, correspond to the closed state.

References

1. Aliev MK, Saks VA. Compartmentalized energy transfer in cardiomyocytes: Use of mathematical modeling for analysis of *in vivo* regulation of respiration. Biophys J 1997;73:428–445. [PubMed: 9199806]

2. O'Rourke B, Ramza BM, Marban E. Oscillations of membrane current and excitability driven by metabolic oscillations in heart cells. Science 1994;265:962–966. [PubMed: 8052856]

3. Ventura-Clapier R, Kuznetsov A, Veksler V, Boehm E, Anflous K. Functional coupling of creatine kinases in muscles: Species and tissue specificity. Mol Cell Biochem 1998;184:231–247. [PubMed: 9746324]

4. Hardie DG, Carling D, Carlson M. The AMP-activated/SNFl protein kinase subfamily: Metabolic sensors of the eukaryotic cell? Annu Rev Biochem 1998;67:821–855. [PubMed: 9759505]

5. Janssen E, Dzeja PP, Oerlemans F, Simonetti AW, Heerschap A, de Haan A, Rush PS, Terjung RR, Wieringa B, Terzic A. Adenylate kinase 1 gene deletion disrupts muscle energetic economy despite metabolic rearrangement. EMBO J 2000;19:6371–6381. [PubMed: 11101510]

6. Dzeja PP, Redfield MM, Burnett JC, Terzic A. Failing energetics in failing hearts. Curr Cardiol Rep 2000;2:212–217. [PubMed: 10980895]

7. Inagaki N, Gonoi T, Clement JP, Namba N, Inazawa J, Gonzalez G, Aguilar-Bryan L, Seino S, Bryan J. Reconstitution of IK$_{ATP}$: An inward rectifier subunit plus the sulfonylurea receptor. Science 1995;270:1166–1170. [PubMed: 7502040]

8. Kaasik A, Veksler V, Boehm E, Novotova M, Minajeva A, Ventura-Clapier R. Energetic crosstalk between organelles: Architectural integration of energy production and utilization. Circ Res 2001;89:153–159. [PubMed: 11463722]

9. Saks VA, Kaambre T, Sikk P, Eimre M, Orlova E, Paju K, Piirsoo A, Appaix F, Kay L, Regitz-Zagrosek V, Fleck E, Seppet E. Intracellular energetic units in red muscle cells. Biochem J 2001;356:643–657. [PubMed: 11368796]

10. Jovanovic A, Jovanovic S, Lorenz E, Terzic A. Recombinant cardiac ATP-sensitive K$^+$ channel subunits confer resistance to chemical hypoxia-reoxygenation injury. Circulation 1998;98:1548–1555. [PubMed: 9769309]

11. Carrasco AJ, Dzeja PP, Alekseev AE, Pucar D, Zingman LV, Abraham MR, Hodgson D, Bienengraeber M, Puceat M, Janssen E, Wieringa B, Terzic A. Adenylate kinase phosphotransfer communicates cellular energetic signals to ATP-sensitive potassium channels. Proc Natl Acad Sci USA 2001;98:7623–7628. [PubMed: 11390963]

12. Yamada K, Ji JJ, Yuan H, Miki T, Sato S, Horimoto N, Shimizu T, Seino S, Inagaki N. Protective role of ATP-sensitive potassium channels in hypoxia-induced generalized seizure. Science 2001;292:1543–1546. [PubMed: 11375491]

13. Inagaki N, Gonoi T, Clement JP, Wang CZ, Aguilar-Bryan L, Bryan J, Seino S. A family of sulfonylurea receptors determines the pharmacological properties of ATP-sensitive K$^+$ channels. Neuron 1996;16:1011–1017. [PubMed: 8630239]

14. Lorenz E, Terzic A. Physical association between recombinant cardiac ATP-sensitive K$^+$ channel subunits Kir6.2 and SUR2A. J Mol Cell Cardiol 1999;31:425–434. [PubMed: 10093054]

15. Clement JP, Kunjilwar K, Gonzalez G, Schwanstecher M, Panten U, Aguilar-Bryan L, Bryan J. Association and stoichiometry of K$_{ATP}$ channel subunits. Neuron 1997;18:827–838. [PubMed: 9182806]

16. Tucker SJ, Gribble FM, Zhao C, Trapp S, Ashcroft FM. Truncation of Kir6.2 produces ATP-sensitive K$^+$ channels in the absence of the sulphonylurea receptor. Nature 1997;387:179–183. [PubMed: 9144288]

17. Drain P, Li L, Wang J. K$_{ATP}$ channel inhibition by ATP requires distinct functional domains of the cytoplasmic C terminus of the pore-forming subunit. Proc NatlAcad Sci USA 1998;95:13953–13958.

18. Shyng SL, Ferrigni T, Nichols CG. Regulation of K$_{ATP}$ channel activity by diazoxide and MgADP: Distinct functions of the two nucleotide binding folds of the sulfonylurea receptor. J Gen Physiol 1997;110:643–654. [PubMed: 9382893]

19. Ashcroft FM, Gribble FM. Correlating structure and function in ATP-sensitive K$^+$ channels. Trends Neurosci 1998;21:288–294. [PubMed: 9683320]

20. Nichols CG, Shyng SL, Nestorowicz A, Glaser B, Clement JP, Gonzalez G, Aguilar-Bryan L, Permutt MA, Bryan J. Adenosine diphosphate as an intracellular regulator of insulin secretion. Science 1996;272:1785–1787. [PubMed: 8650576]

21. Matsuo M, Tanabe K, Kioka N, Amachi T, Ueda K. Different binding properties and affinities for ATP and ADP among sulfonylurea receptor subtypes, SUR1, SUR2A, and SUR2B. J Biol Chem 2000;275:28757–28763. [PubMed: 10893240]

22. Bienengraeber M, Alekseev AE, Abraham MR, Carrasco AJ, Moreau C, Vivaudou M, Dzeja PP, Terzic A. ATPase activity of the sulfonylurea receptor: A catalytic function for the K-ATP channel complex. FASEB j 2000;14:1943–1952. [PubMed: 11023978]

23. Zingman LV, Hodgson DM, Bienengraeber M, Kargcr AB, Kathmann EC, Alekseev AE, Terzic A. Tandem function of nucleotide binding domains confers competence to sulfonylurea receptor in gating ATP-sensitive K$^+$ channels. J Biol Chem 2002;277:14206–14210. [PubMed: 11825892]

24. Zingman LV, Alekseev AE, Bienengraeber M, Hodgson D, Karger AB, Dzeja PP, Terzic A. Signaling in channel/enzyme multimers: ATPase transitions in SUR module gate ATP-sensitive K$^+$ conductance. Neuron 2001;31:233–245. [PubMed: 11502255]

25. Ledcrer WJ, Nichols CG. Nucleotide modulation of the activity of rat heart ATP-sensitive K$^+$ channels in isolated membrane patches. J Physiol 1989;419:193–211. [PubMed: 2621629]

26. Weiss JN, Venkatesh N, Lamp ST. ATP-sensitive K$^+$ channels and cellular K$^+$ loss in hypoxic and ischaemic mammalian ventricle. J Physiol 1992;447:649–673. [PubMed: 1593462]

27. Bittl JA, DeLayre J, Ingwall JS. Rate equation for creatine kinase predicts the *in vivo* reaction velocity: ^{31}P NMR surface coil studies in brain, heart, and skeletal muscle of the living rat. Biochemistry 1987;26:6083–6090. [PubMed: 3689762]

28. Saks VA, Aliev MK. Ts there the creatine kinase equilibrium in working heart cells? Biochem Biophys Res Commun 1996;227:360–367. [PubMed: 8878521]

29. Weiss JN, Lamp ST. Glycolysis preferentially inhibits ATP-sensitive K$^+$ channels in isolated guinea pig cardiac myocytes. Science 1988;238:67–69. [PubMed: 2443972]

30. Weiss JN, Venkatesh N. Metabolic regulation of cardiac ATP-sensitive K$^+$ channels. Cardiovasc Drugs Ther 1993;7:499–505. [PubMed: 8251419]

31. Lederer WJ, Niggli E, Hadley RW. Sodium-calcium exchange in excitable cells: Fuzzy space. Science 1990;248:283. [PubMed: 2326638]

32. Dzeja PP, Terzic A. Phosphotransfer reactions in the regulation of ATP-sensitive K$^+$ channels. FASEB J 1998;12:523–529. [PubMed: 9576479]

33. Elvir-Mairena JR, Jovanovic A, Gomez LA, Alekseev AE, Terzic A. Reversal of the ATP-liganded state of ATP-sensitive K$^+$ channels by adenylate kinase activity. J Biol Chem 1996;271:31903–31908. [PubMed: 8943234]

34. Abraham MR, Selivanov VA, Hodgson DM, Pucar D, Zingman LV, Wieringa B, Dzeja PP, Alekseev AE, Terzic A. Coupling of cell energetics with membrane metabolic sensing. Integrative signaling through creatine kinase phosphotransfer disrupted by M-CK gene knock-out. J Biol Chem 2002;277:24427–24434. [PubMed: 11967264]

35. Dzeja PP, Vitkevicius KT, Redfield MM, Burnett JC, Terzic A. Adenylate kinase-catalyzed phosphotransfer in the myocardium: Increased contribution in heart failure. Circ Res 1999;84:1137–1143. [PubMed: 10347088]

36. Olson LK, Schroeder W, Robertson RP, Goldberg ND, Walseth TF. Suppression of adenylate kinase catalyzed phosphotransfer precedes and is associated with glucose-induced insulin secretion in intact HITT15 cells. J Biol Chem 1996;271:16544–16552. [PubMed: 8663240]

37. Sasaki N, Sato T, Marban E, O'Rourke B. ATP consumption by un-coupled mitochondria activates sarcolemmal K$_{ATP}$ channels in cardiac myocytes. Am J Physiol 2001;280:H1882–H1888.

38. Crawford RM, Ranki HJ, Bolting CH, Budas GR, Jovanovic A. Creatine kinase is physically associated with the cardiac ATP-sensitive K$^+$ channel *in vivo*. FASEB J 2002;16:102–104. [PubMed: 11729098]

39. Nichols CG, Lederer WJ. The regulation of ATP-sensitive K$^+$ channel activity in intact and permeabilized rat ventricular myocytes. J Physiol 1990;423:91–110. [PubMed: 2388163]

40. Chazov, El; Smirnov, VN.; Saks, VA.; Rosenshtraukh, LV.; Lipina, NV.; Levitsky, DO. Energy metabolism and ion fluxes across cardiac membranes. Adv Myocardiol 1980;1:139–153. [PubMed: 6248931]

41. Kabakov AY. Activation of K$_{ATP}$ channels by Na/K pump in isolated cardiac myocytes and giant membrane patches. Biophys J 1998;75:2858–2867. [PubMed: 9826607]

42. Rich TC, Fagan KA, Nakata H, Schaack J, Cooper DM, Karpen JW. Cyclic nucleotide-gated channels colocalize with adenylyl cyclase in regions of restricted cAMP diffusion. J Gen Physiol 2000;116:147–161. [PubMed: 10919863]

43. Pucar D, Dzeja PP, Bast P, Juranic N, Macura S, Terzic A. Cellular energetics in the preconditioned state: Protective role for phosphotransfer reactions captured by ^{18}O$_O$-assisted ^{31}P NMR. J Biol Chem 2001;276:44812–44819. [PubMed: 11583991]

44. Lawson JW, Veech RL. Effects of pH and free Mg^{2+} on the K$_{eq}$ of the creatine kinase reaction and other phosphate hydrolyses and phosphate transfer reactions. J Biol Chem 1979;254:6528–6537. [PubMed: 36398]

45. Jacobus WE. Theoretical support for the heart phosphocreatine energy transport shuttle based on the intracellular diffusion limited mobility of ADP. Biochem Biophys Res Commun 1985;133:1035–1041. [PubMed: 4084301]

46. Dzeja PP, Zeleznikar RJ, Goldberg ND. Suppression of creatine kinasecatalyzed phosphotransfer results in increased phosphoryl transfer by adenylate kinase in intact skeletal muscle. J Biol Chem 1996;271:12847–12851. [PubMed: 8662747]

47. Pucar D, Janssen E, Dzeja PP, Juranic N, Macura S, Wieringa B, Terzic A. Compromised energetics in the adenylate kinase AK1 gene knockout heart under metabolic stress. J Biol Chem 2000;275:41424–41429. [PubMed: 11006295]

48. Dzeja PP, Bortolon R, Perez-Terzic C, Holmuhamedov EL, Terzic A. Energetic communication between mitochondria and nucleus directed by catalyzed phosphotransfer. Proc Natl Acad Sci USA 2002;99:10156–10161. [PubMed: 12119406]

49. Decking UK, Reffelmann T, Schrader J, Kammermeier H. Hypoxia-induced activation of K_{ATP} channels limits energy depletion in the guinea pig heart. Am J Physiol 1995;269:H734–H742. [PubMed: 7653639]

50. Zingman LV, Hodgson DM, Bast PH, Kane GC, Perez-Terzic C, Gumina RJ, Pucar D, Bienengraeber M, Dzeja PP, Miki T, Seino S, Alekseev AE, Terzic A. Kir6.2 is required for adaptation to stress. Proc Natl Acad Sci USA 2002;99:13278–13283. [PubMed: 12271142]

51. Pucar D, Bast P, Gumina RJ, Lim L, Drahl C, Juranic N, Macura S, Janssen E, Wieringa B, Terzic A, Dzeja PP. Adenylate kinase AK1 knockout heart: Energetics and functional performance under ischemiareperfusion. Am J Physiol 2002;283:H776–H782.

52. Ghosh MC, Jencks WP. Phosphorylation of the sodium-potassium adenosinetriphosphatase with adenosine triphosphate and sodium ion that requires subconformations in addition to principal El and E2 conformations of the enzyme. Biochemistry 1996;35:12587–12590. [PubMed: 8823196]

53. Joubert F, Mazet JL, Mateo P, Hoerter JA. ^{31}P NMR detection of subcellular creatine kinase fluxes in the perfused rat heart: Contractility modifies energy transfer pathways. J Biol Chem 2002;277:18469–18476. [PubMed: 11886866]

54. Gogelein H, Hartung J, Englert HC. Molecular basis, pharmacology and physiological role of cardiac K_{ATP} channels. Cell Physiol Biochem 1999;9:227–241. [PubMed: 10575200]

55. Kusuoka H, Inoue M, Tsuneoka Y, Watari H, Hori M, Abe H. Augmented energy consumption during early systole as a mechanism of cyclical changes in high-energy phosphates in myocardium assessed by phosphorus nuclear magnetic resonance. Jpn Circ J 1985;49:1099–107. [PubMed: 4087340]
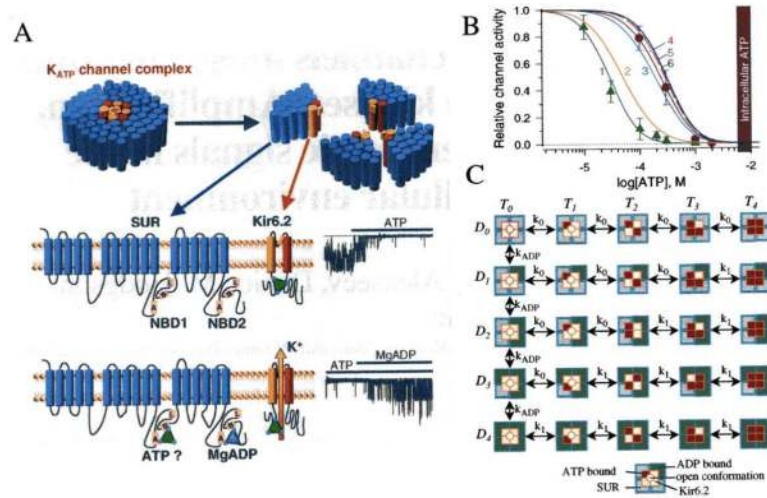
Fig. 1.
Stoicheometry and allosteric nucleotide-dependent gating of K_{ATP} channels. (A) The K_{ATP} channel is an octameric complex composed of four pore-forming Kir6.2 subunits and four associated regulatory SUR subunits. Kir6.2 is formed by two transmembrane domains flanking a pore region. SUR is characterized by two cytosolic nucleotide-binding domains (NBD1 and NBD2) which contain highly-conserved Walker A and Walker B motifs as well as a linker (L) region. Interaction of ATP (green triangle) with Kir6.2 induces pore closure. Upper channel record demonstrates ATP-induced K_{ATP} channel inhibition. MgADP (blue triangle) at NBD2 antagonizes ATP-induced pore inhibition, with an apparent requirement of ATP at NBD1. Lower channel record demonstrates MgADP-induced reduction of ATP-induced K_{ATP} channel inhibition leading to channel opening. (B) MgADP antagonizes ATP-induced inhibition of cardiac K_{ATP} channels. In excised patches, the ATP sensitivity of K_{ATP} channels was defined by an IC_{50} of 27 ± 5 mM in the absence (triangles) vs. 270 ± 19 μM in the presence (circles) of 100 μM ADP. Relative channel activity (curves) constructed based on an allosteric model of nucleotide-dependent K_{ATP} channel gating (C; see Appendix), and expressed as a probability for the channel to be in an open state (columns T_0-T_1. In the absence of ADP, channels adopt the highest sensitivity to ATP (row D_0) defined solely by the microscopic dissociation constant $k_0 = 45$ μM (curve 1). At saturating ADP concentrations, K_{ATP} channels convert to channel species with the lowest ATP sensitivity (row D_4) defined solely by $k_1 = 450$ μM (curve 4). k_{ADP} (12.5 μM) was determined at different concentrations of ADP (curve 1: 0; 2: 10; 3: 50; 4: 100; 5: 500; 6: 1000 μM ADP).

Open cell-attached patch configuration
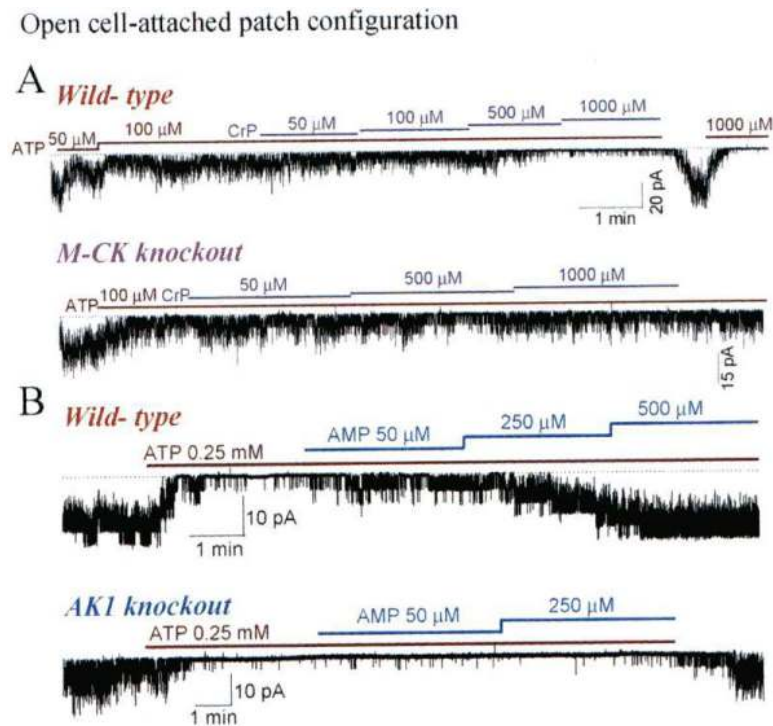
Fig. 2.
K$_{ATP}$ channels communicate with intracellular phosphotransfer systems. To maintain the relative integrity of the cellular infrastructure, K$_{ATP}$ channel activity was recorded in the open-cell attached patch mode in cardiac cells from wild-type and *M-CK* or *AK1*-deficient mice (see [22,34]). (A) CrP-dependent regulation of K$_{ATP}$ channels is lost in M-CK-knockout cardiac cells. While in the wild-type, CrP enhanced K$_{ATP}$ channel inhibition by 100 μM ATP (upper trace), in M-CK knockouts (lower trace) the creatine kinase substrate was deprived of a significant effect. Temperature was 31°C. Adapted from [34]. (B) AMP-dependent regulation of K$_{ATP}$ channels is lost in AK1 -knockout cardiac cells. K$_{ATP}$ channel recordings demonstrate activation of ATP-inhibited channels following application of AMP, an adenylate kinase substrate (upper trace), but absence of AMP effect in cardiomyocytes from AK 1 -knockout hearts. Measurements were at room temperature. Adapted from [11].
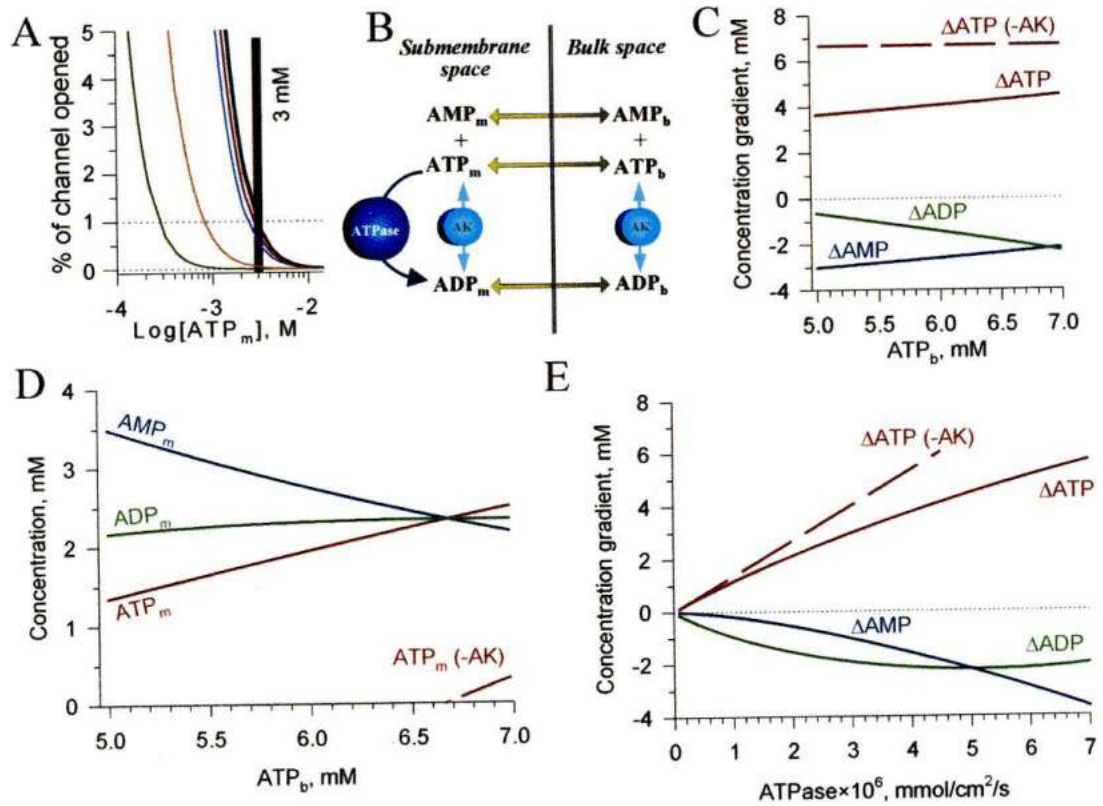
Fig. 3.
Adenylate kinase diminishes nucleotide gradients between cellular compartments. (A) ATP-dependence of relative channel activity constructed based on the allosteric model of K_{ATP} channel gating ($k_0 = 10$ μM, $k_1 = 450$ μM, $k_{ADP} = 12.5$ μM; see Appendix) at (from left to right) 0,0.01, 0.05, 0.1, 0.5 and 1.0 mM MgADP, with further addition of ADP not shifting the curve. Vertical bar indicates concentration of ATP (3 mM), at which at least 1 % of K_{ATP} channel population could be opened at saturated ADP level. (B) The model used to estimate diffusion coefficient for adenine nucleotides in submembrane space (Eqs 1-6). ATPase in submembrane space creates nucleotide gradients modified by the AK reaction operating at a presumed equilibrium in both compartments. Gradients cause nucleotide diffusion fluxes (horizontal arrows) over diffusion barrier according to Fick's law. The diffusion coefficient 1.5 10^{-11} cm^2/s was calculated (Eqs 1, 2 and 4) based on the assumption that at 7 mM of total nucleotides, 6.0 mM of bulk ATP ($[ATP]_b$) and a membrane ATPase activity of a working heart (4.7 10^{-6} μmol/cm^2/s), submembrane ATP ($[ATP]_m$) levels must drop to 3 mM in order to secure minimum K_{ATP} channel activity (1% of the channel population) sufficient for changes in cardiac membrane excitability. (C) Differences in ATP, ADP and AMP concentrations (ΔATP, ΔADP and ΔAMP) between the bulk and submembrane space estimated using Eq. 6 as function of bulk ATP. (D) Expected submembrane nucleotide concentration corresponding to nucleotide concentration gradients presented in (C). (E) Differences in nucleotide concentrations between the bulk and sub-membrane space computed at various membrane ATPase activities; (-AK) indicates curves constructed assuming absence of AK activity.
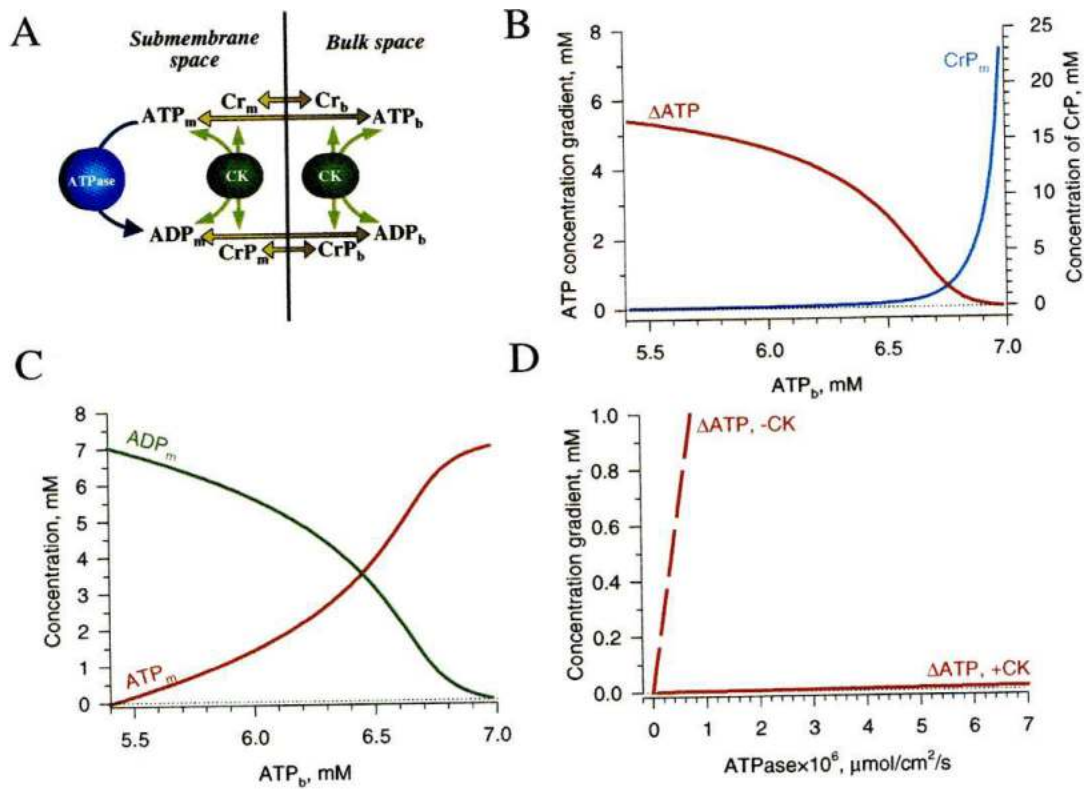
Fig. 4.
Creatine kinase as a submembrane amplifier of cytosolic changes in ATP and ADP. (A) Model of CrP/CK - facilitated diffusion for adenine nucleotide (Eqs 7-13). ATPase and creatine kinase reactions (assumed at equilibrium) in the submembrane space create nucleotide and creatine gradients that cause diffusional fluxes (horizontal arrows) according to Fick's law. (B) Profiles of ΔATP and submembrane concentration of creatine phosphate ($[CrP]_m$) constructed based on Eq. 13 as a function of bulk ATP ($[ATP]_b$), at 7 mM total nucleotide content, 40 mM total Cr/CrP level, ATPase flux 4.7 10^{-6} umol/cm^2/s, diffusion coefficient 2.25 10^{-11} cm^2/s, and the equilibrium constant for the CK reaction $K_{CK} = 160$. (C) The sub-membrane concentration of ATP and ADP at the parameters used in (B). (D) Differences in nucleotide concentrations between bulk and sub-membrane space at various membrane ATPase activities, $[ATP]_b = 6.99$ mM in the absence (-CK) or presence (+CK) of CK activity.
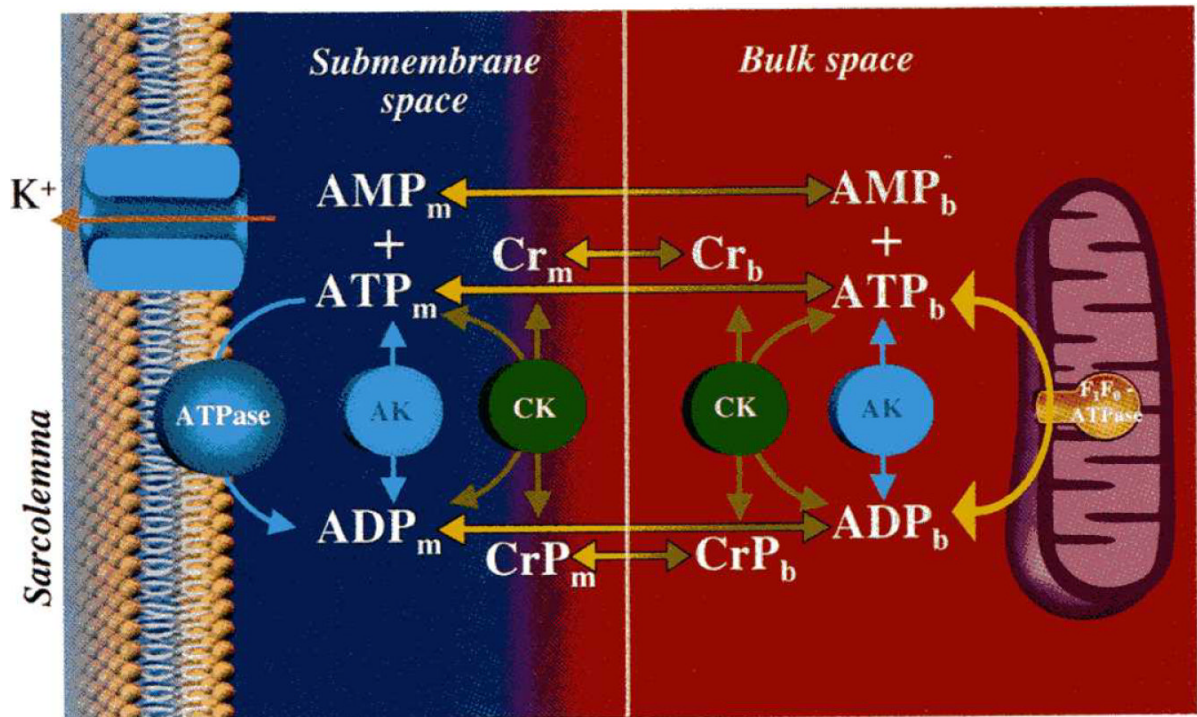
Fig. 5.
Adenine nucleotide diffusion facilitated by the CrP/CK system in the presence of AK.
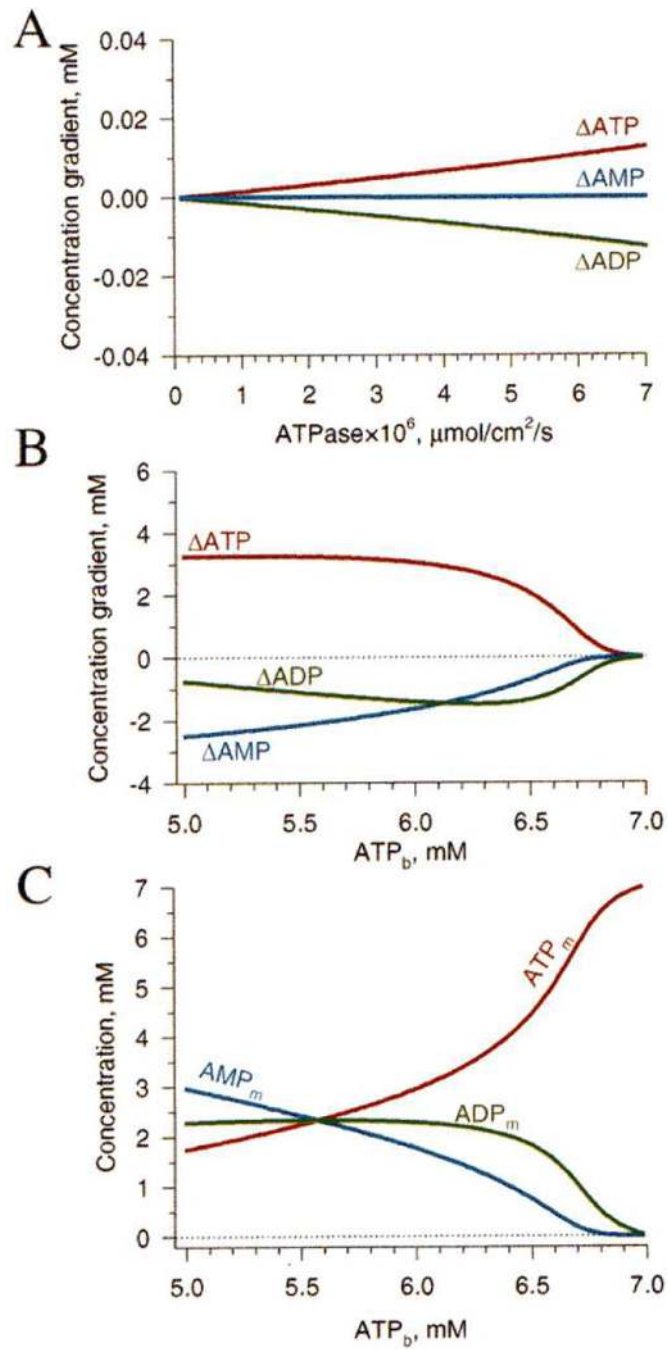
Fig. 6.
Regulation of adenine nucleotides by coactivc creatine and adenylate kinases. (A) Differences in nucleotide concentrations between hulk and sub-membrane space at various membrane ATPase activities obtained by resolving the system of Eqs 2,4,5,8,9, 11,12, and 14 with corresponding parameters as in Figs 3E and 4D. (B) Differences in nucleotide concentrations between bulk and submembrane compartments at membrane ATPase activity = $4.7\ 10^{-6}$ µmol/cm^2/s and various $[ATP]_b$. (C) Submembrane nucleotidc concentrations that correspond to ΔATP, ΔADP, and ΔAMP shown in (B).
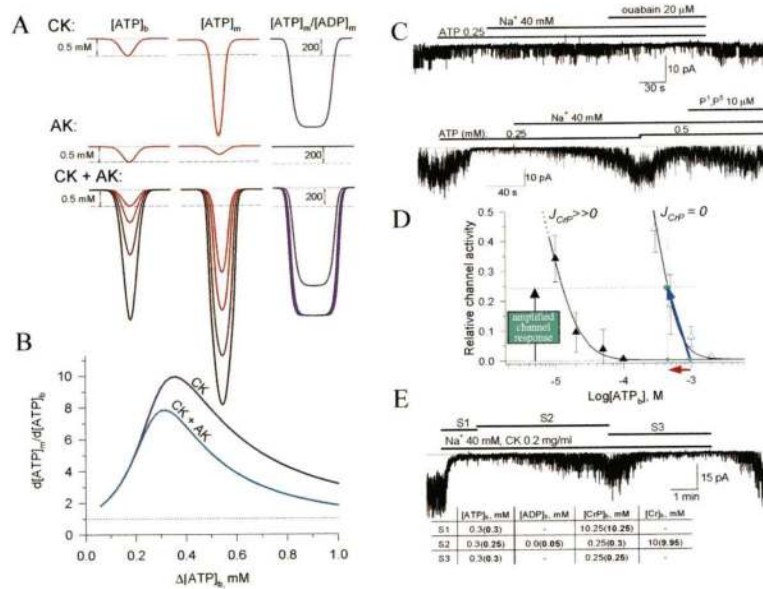
Fig. 7.
Amplification and tuning of energetic signals by CK and AK. Energetic signal was simulated as a slow-rate, gaussian, dip in $[ATP]_b$. (A) CK amplifies a 0.5 mM drop in $[ATP]_b$ into a ~ 6 time higher change in $[ATP]_m$ corresponding to a significant response in the $[ATP]_m/[ADP]_m$ ratio (upper row). AK provides a ~ 2 times attenuation of $[ATP]_m$ in response to the 0.5 mM drop in $[ATP]_b$, insufficient to induce significant changes in the $[ATP]_m/[ADP]_m$ ratio (middle row). Coactive AK and CK provide significant amplification of a $[ATP]_b$ signal, yet doubling in $[ATP]_b$ signals (0.5, 1, 2, and 4 mM dips) transmit into an amplified and modulated (2.6, 3.7, 5.1, and 6.6 mM, respectively) response in $[ATP]_m$ and a cut-off of $[ATP]_m/[ADP]_m$ ratio (lower row). Note that higher signals undergo a lower amplification, an effect enhanced by AK. (B) Effectiveness of signal transmission represented as a derivative of changes in $[ATP]_m$ over $[ATP]_b$ for CK alone and co-active CK and AK systems. Dotted line corresponds to a passive signal response in the absence of systems catalyzing phosphotransfer reactions. (C) In rat cardiomyocytes, in the open cell-attached mode of the patch-clamp technique, ATP-induced K_{ATP} channel inhibition was antagonized by activation of membrane Na^+/K^+ ATPase following application of 40 mM of NaCl. Ouabain, an inhibitor of the Na^+/K^+ pump, reversed ATP-induced channel closure (upper trace). Di(adenosine-5′) pentaphosphate (P^1,P^5), a selective AK inhibitor, produced additional opening of K_{ATP} channels under active membrane Na^+/K^+ ATPase, preventing AK scavenging of ADP and support of ATP levels in the submembrane compartment. (D) Concentration-response curves defining ATP-induced K_{ATP} channel inhibition measured from guinea-pig cardiomyocytes in open cell-attached mode in the absence ($J_{CrP} = 0$, open triangles) and in the presence of 1 mM CrP ($J_{Crp} >> 0$, closed triangles). Solid curves were constructed based on the allosteric model of channel regulation (with $k_0 = 10$ μM, $k_1 = 450$ μM, $k_{ADP} = 12.5$ μM), in conjunction with nucleotide diffusion, J_{ATPase} and creatine kinase (J_{CK}) fluxes (see [34]). Activation of CK flux produced a significant left-shift of ATP-induced K_{ATP} channel inhibition from $IC_{50} = 270 \pm 2$ μM at $J_{Crp} = 0$ to $IC_{50} = 7 \pm 1$ μM at $J_{CrP} >> 0$. Following changes in $[ATP]_b$, without changes in J_{CrP}, K_{ATP} channels remain closed in accord with a higher ATP sensitivity (red arrow). Assuming that the proposed shift in $[ATP]_b$ corresponds to complete suppression of J_{CrP}, K_{ATP} channel activity can be determined as a transition to the curve defining lower ATP sensitivity (blue arrow) resulting in amplified changes in open channel probability. (E) Transmission of an amplified energetic signal from the bulk space to the K_{ATP} channel site by altered CK flux was assessed in mice cardiomyocytes, under active membrane Na^+/K^+ ATPase,

in open cell-attached patches. S1, S2 and S3 solutions, with compositions presented in the table, simulated different values for CK fluxes. In the Table, applied concentrations are in normal typeface, whereas actual concentrations defined according to the reaction equilibrium (Eq. 9) are bold in parentheses. In order to secure reaction equilibrium in the bulk space, all solutions were supplemented with exogenous CK (170-200 U/ml) in addition to intracellular CK. Vigorous K_{ATP} channel activity was readily inhibited by high J_{CrP} simuxlated by S1 at 0.3 mM $[ATP]_b$. Low J_{CrP} (solution S2) led to K_{ATP} channel opening amplifying minor changes in $[ATP]_b$ and $[ADP]_b$ within the submembrane compartment. The amount of CrP used in S2 was sufficient to reverse K_{ATP} channel inhibition in the absence of Cr (solution S3). Measurements were performed at 60 mV, and 31 ± 1°C.
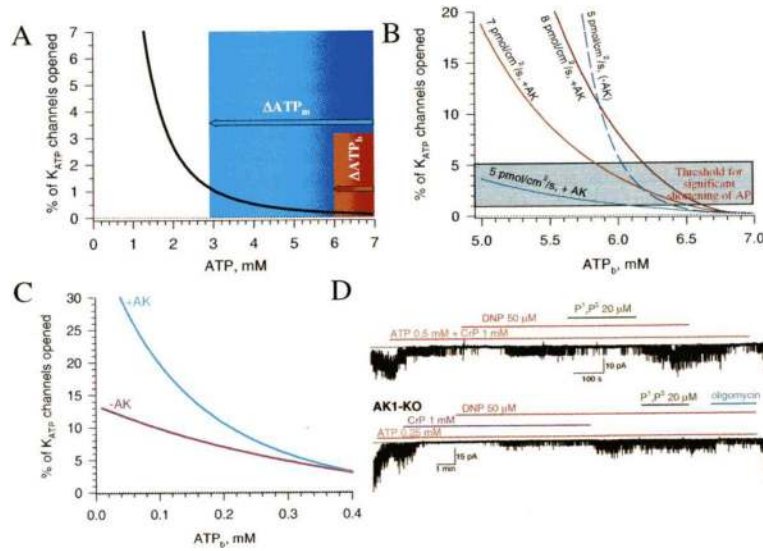
Fig. 8.

K_{ATP} channels as sensors of metabolic signals transmitted over diffusion barrier by the creatine and adenylate kinases. (A) Solid curve depicts regulation of K_{ATP} channels by submembrane nucleotides, calculated based on the allosteric model (see Appendix) at 7 mM of total nucleotide and various $[ATP]_b$. In the absence of stress co-active CK and AK essentially void nucleotide gradients, equalizing $[ATP]_b$ and $[ATP]_m$, and keeping K_{ATP} channels closed. A stress-induced 1 mM drop of $[ATP]_b$ (ΔATP_b, small bar), would be amplified into a dramatic drop in $[ATP]_m$ (ΔATP_m, large bar) permitting opening of > 1% of K_{ATP} channels (intersection of the right edge of the bar for ΔATP_m with solid curve). (B) Threshold for significant shortening of cardiac action potential represented as a bar filling the 1-5% range of open K_{ATP} channels. Channel activity calculated based on the allosteric model of channel regulation by submembrane nucleotides at various $[ATP]_b$ and different membrane ATPase activities. In the absence of adenylate kinase (-AK) the extremely steep nucleotide-dependent channel regulation (dashed line) would expose cells to excessive K_{ATP} current at relatively modest changes in $[ATP]_b$. (C) AK system may favor K_{ATP} channel openings at active bulk ATPase, i.e. following vigorous mitochondria uncoupling, when $[ATP]_m > [ATP]_b$. Such conditions require the support of $[ATP]_m$ which was simulated through diffusional flux of ATP (J^0_{ATP}) and CrP (J^0_{CrP}) into the submembrane space from a third compartment with a constant level of $[ATP]^0 = 0.5$ mM and $[CrP]^0 = 1$ mM. Thus, at steady state:

$$J^0_{ATP} + J^0_{CrP} = -J_{AMP} + J_{ATP} + J_{CrP}, \tag{15}$$

where

$$J^0_{ATP} = \frac{-DS}{\Delta X} \left([ATP]^0 - [ATP]m \right),$$

$$J^0_{CrP} = \frac{-DS}{\Delta X} \left([CrP]^0 - [CrP]m \right)$$

whereas other fluxes defined from Eqs 2 and 8. The relation between fluxes (Eq. 15) is similar to Eq. 14, ignoring submembrane ATPase activity (J_{ATPase}). The percentage of opened K_{ATP} channels was estimated using the allosteric model for channel regulation by submembrane nucleotide levels, that were calculated for co-active CK and AK activities (+AK, Eqs 2, 4, 5, 8, 9, 11, 12, and 15), *vs.* CK alone (-AK, Eqs 8, 9, 11, 12, and 15) at various bulk ATPase-induced drop of $[ATP]_b$. (D) Activity of K_{ATP} channels measured in cardiomyocytes isolated from wile-type (upper trace) and AK1-deficient (AK1-KO, lower trace) mice under simulated conditions described above (C). To preserve intracellular catalytic systems recording were performed in the open cell-attached mode at 30°C [see 11]. In wild-type, P^1,P^5 inhibited adenylate kinase activity and effectively inhibited DNP-induced K_{ATP} channel openings ($[ATP]^0 = 0.5$ mM, $[CrP]^0 = 1$ mM) indicating involvement of the AK system in channel openings (note, that membrane ATPase activity in resting cardiomyocytes, as in such experimental conditions, is much lower in comparison with cells in working heart). In AK1-knockout cardiomyocytes, the K_{ATP} channel response to DNP-induced mitochondrial ATPase activation was blunted and sensitive to oligomycin, but insensitive to P^1,P^5 ($[ATP]^0 = 0.25$ mM, $[CrP]_0 = 1$ mM; [adapted from 11]).